Tetrahedron 68 (2012) 767–773

Contents lists available at SciVerse ScienceDirect

Tetrahedron

journal homepage: www.elsevier.com/locate/tet

Dipolar organic pyridyl dyes for dye-sensitized solar cell applications

Hsien-Hsin Chou [a], Chih-Yu Hsu [a], Ying-Chang Hsu [a], Yu-Sheng Lin [b], Jiann T. Lin [a,*], Chiitang Tsai [b,*]

[a] Institute of Chemistry, Academia Sinica, No. 128, Sec. 2, Academia Road, Taipei 115, Taiwan
[b] Department of Chemistry, Chinese Culture University, Taipei 320, Taiwan

ARTICLE INFO

Article history:
Received 28 June 2011
Received in revised form 22 September 2011
Accepted 11 October 2011
Available online 13 November 2011

Keywords:
Dye-sensitized solar cells
Pyridine
Dipolar compounds
Metal-free dyes

ABSTRACT

New dipolar dyes containing arylamine as the electron donor, 2-cyanoacrylic acid as the acceptor, and a conjugated spacer with incorporation of 2,5-pyridyl entity have been synthesized. Photophysical and electrochemical measurements, and theoretical computation were carried on these dyes. The solar cell devices using these dyes as the sensitizers exhibited light-to-electricity efficiencies in the range of 4.28–5.27%, which reaches 60–72% of N719-based device fabricated and measured under similar conditions. Better DSSC performance can be achieved with the dye where pyridine group is attached to thienyl or fluorenyl group because of favorable resonance energy and/or coplanarity for more effective charge transfer.

1. Introduction

Since the beginning of the 21st century, depletion of fossil fuel reserve and global warming have become important worldwide issues, which boost up tremendous growth of investigations on environmental friendly new energy sources as well as more efficient energy conversion and storage. Solar energy is very attractive because of its environmental benign and endless supply. Unfortunately, up to date the crystalline and thin-film silicon-based photovoltaics still suffer from major drawback, that is, request of high purity materials and therefore accompanying with high cost. Dye-sensitized solar cells (DSSCs) are considered to be attractive alternative of low cost solar cells since Grätzel's pioneer work.[1] An ideal molecule to be used as the sensitizer for DSSCs requires a larger electronic absorption coefficient, broad spectral coverage even to near infrared region and good stability.[2] At present, the solar cell device fabricated with ruthenium-based polypyridine complexes records the highest conversion efficiency above 11%.[3] Nevertheless, the rather expensive cost of transition metal coupled with lower absorption coefficient due to MLCT nature push researchers searching for metal-free dyes as alternatives. Coumarin-,[4] indoline-,[5] cyanine-,[6] hemicyanine-,[7] triphenylamine-,[8] tetrahydroquinoline-,[9] truxene-,[10] polyene-,[11] thienothiophene-,[12] oligothiophene-,[13] furan-,[14] and pyrrole-based[15] metal-free dyes have been reported for various purposes to enlarge cell performances. Dyes having 4,4′-bis(hexyloxylphenyl)aminobenzene as the donor, 2-cyanoacrylic acid as the acceptor and oligothiophenes as the conjugated spacer has the conversion efficiency at ~10%, which is the best performance ever reported.[16]

We have been interested in push–pull type[17] sensitizers using arylamine as the electron donor[18] and 2-cyanoacrylic acid as the electron acceptor. In one of our reports, dipolar organic dyes with a fluorene and a heteroaromatic ring in the conjugated spacer exhibited high cell efficiencies reaching ~95% of N719-based (N719=bis(tetrabutyl-ammonium)-*cis*-di(thiocyanato)-*N*,*N*′-bis(4-carboxylato-4′-carboxylic acid-2,2′-bipyridine)ruthenium(II)) standard cell.[19] However, these sensitizers have relatively short absorption wavelengths (~420 nm). In comparison, sensitizers with implanted benzothiadiazole or benzoselenadiazole in the spacer were found to have much longer absorption wavelengths.[8a,20a–c] Nevertheless, the dyes developed by us have the cell efficiency reaching only ≤71% of N3-based device.[8a] Sensitizers with electron-withdrawing cyanovinyl unit in the conjugated spacer also have long absorption wavelengths (up to 578 nm), but relatively lower efficiencies reaching only ≤69% of N719-based standard cell.[20d] Density functional calculations indicated that charge trapping occurred at the cyanovinyl group upon vertical excitation, which hampered efficient electron injection from the sensitizer to the TiO_2 nanoparticles. We therefore searched for other electron-withdrawing entity as the building block of the spacer in the hope of red shifting the absorption spectra without charge trapping. We then turned our attention to pyridine, which is more electron deficient than thiophene and benzene, and has resonance energy (32 kcal mol^{-1}) lying between the two (thiophene: 29; benzene: 36 kcal mol^{-1}).[21] To our knowledge, there was only two reports on metal-free pyridine-based

* Corresponding authors. Tel.: +886 2 27898522; fax: +886 2 27831237; e-mail addresses: hhchou@chem.sinica.edu.tw (H.-H. Chou), jtlin@chem.sinica.edu.tw (J.T. Lin).

0040-4020/$ – see front matter © 2011 Elsevier Ltd. All rights reserved.
doi:10.1016/j.tet.2011.10.038

sensitizers.[22] In this paper, we report new series of dipolar metal-free compounds and DSSCs based on these sensitizers.

2. Results and discussions

2.1. Synthesis of the materials

New dipolar dyes shown in Fig. 1 were prepared in moderate to good yields. Scheme 1 illustrates the synthetic protocol of the new compounds. Suzuki coupling[23] of the arylamino-substituted arylboronic acids and 2-bromo-5-pyridylaldehyde to give the dipolar aldehyde compounds **1a**–**4a** in moderate yields. Similar coupling of the arylamino-substituted arylboronic acid and 2-bromothiazole followed by formylation of thiazole derivative gave aldehyde derivative **5a**. Finally, condensation of cyanoacetic acid and **1a**–**5a** with cyanoacetic acid yielded the desired products **Y1**–**Y5**. The dyes are colored in intense red and stable both in solid form and in solution.

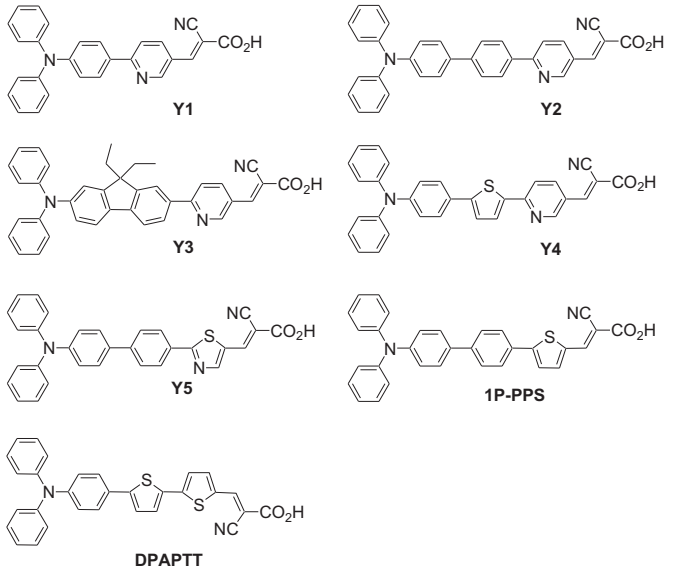

Fig. 1. The structures of the dyes.

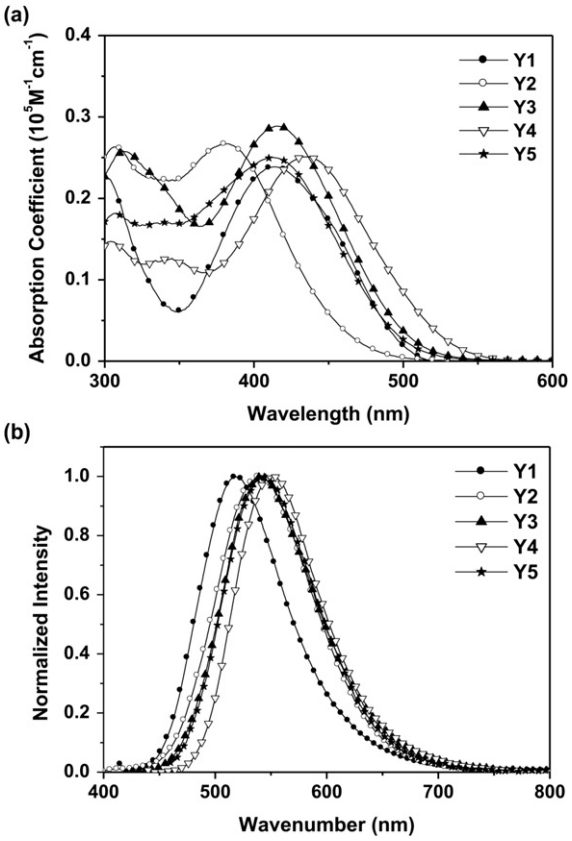

Fig. 2. Absorption (a) and emission (b) spectra of the dyes recorded in THF.

attributable to localized π–π* transition; another band at the region from 382 to 436 nm is attributed to the superposition of more delocalized π–π* and charge-transfer transitions. The λ_{max} value of dye **Y3** (416 nm) is greater than that of **Y2** (382 nm), indicating that the large twist angle between the two internal phenyl groups in **Y2** deteriorates effective π-conjugation. **Y1** has a similar absorption wavelength (415 nm) as **Y3** despite of its shorter conjugation spacer. Clearly, **Y1** has more charge-transfer character than **Y3** (see computation results).

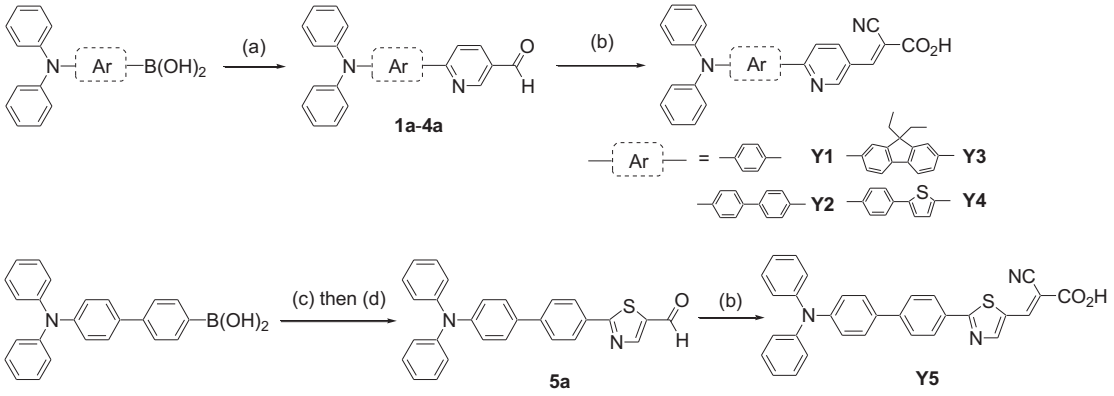

Scheme 1. (a) 2-Bromo-5-pyridylaldehyde, cat. $Pd(PPh_3)_4$, Na_2CO_3, EtOH, toluene, 85 °C (b) $NCCH_2CO_2H$, cat. piperidine, CH_3CN, 80 °C (c) 2-bromothiazole, cat. $Pd(PPh_3)_4$, Na_2CO_3, toluene, EtOH, 85 °C (d) i. *n*-BuLi, THF, −78 °C; ii. DMF.

2.2. Photophysical properties

Representative absorption and emission spectra of the dyes in THF are displayed in Fig. 2 and the data are compiled in Table 1. As shown in Fig. 2a, the dyes exhibit two intense absorption bands in UV–vis region upon photoexcitation: the absorption band lies at 300–312 nm is

Further red shift of the absorption spectra can be achieved by replacing the internal phenyl unit with a thienyl group, as in **Y4** (436 nm). Such an outcome may be attributed to the smaller resonance energy of thiophene than benzene ring, which facilitates the charge transfer from the donor to the acceptor. It is interesting to note that replacement of the pyridine ring in **Y2** with the more electron-deficient

Table 1
Electrooptical parameters of the dyes[a] and performance parameters of DSSCs fabricated with these dyes[e]

	λ_{abs} (10^{-4} ε) [nm]	λ_{em} [nm]	ν_{st} [cm^{-1}]	$E^{ox}_{1/2}$ (ΔEp)[b] [mV]	HOMO/LUMO [eV]	E_{0-0}[c] [eV]	E_{0-0}*[d] [V]	V_{OC} [V]	J_{SC} [$mAcm^2$]	η [%]	FF	R_{ct}[f] [Ω]	Dye loading [10^{-7} mol cm^{-2}]
Y1	300 (2.27), 415 (2.39)	519	4829	611 (233)	5.81/3.38	2.43	−1.12	0.67	10.20	4.67	0.68	15.9	3.18
Y2	308 (2.64), 382 (2.67)	539	7625	544 (205)	5.74/3.08	2.66	−1.42	0.65	9.72	4.28	0.68	17.3	4.90
Y3	312 (2.58), 416 (2.89)	541	5554	505 (113)	5.71/3.24	2.47	−1.26	0.66	10.71	4.87	0.69	16.5	7.59
Y4	304 (1.47), 345 (1.27), 436 (2.51)	553	4853	518 (126)	5.72/3.42	2.30	−1.08	0.63	12.33	5.27	0.68	9.8	5.29
Y5	308 (1.82), 413 (2.50)	542	5763	575 (160)	5.78/3.31	2.47	−1.19	0.68	9.90	4.61	0.68	11.6	3.78
N719								0.70	15.08	7.18	0.68	—	—

[a] All experiments were conducted in THF. λ_{abs}: absorption wavelength; ε: extinction coefficient; λ_{em}: emission wavelength; ν_{st}: Stokes shift.
[b] Scan rate, 100 mV/s; electrolyte, (n-Bu)$_4$NPF$_6$; ΔE_p is the separation between the anodic and cathodic peaks. Potentials are quoted with reference to the internal ferrocene standard ($E^{ox}_{1/2}$=+212 mV vs Ag/AgNO$_3$). The HOMO and LUMO energies are calculated using formula HOMO=5.2+($E_{1/2}$−E_{Fc}) and LUMO=HOMO−E_{gap}, where 5.2 refers to energy level of ferrocene in vacuo.
[c] The optical bandgap (E_{0-0}) defines the onset value of lowest-energy absorption peak.
[d] The bandgap E_{0-0}* defines the reduction potential corresponding to NHE using the formula E_{0-0}*=LUMO−4.5 V.
[e] Experiments were conducted using TiO_2 photoelectrodes with approximately 18 μm thickness and 0.25 cm^2 working area on the FTO (15 Ω/sq.) substrates.
[f] Charge transfer resistances (R_{ct}) were obtained from the radius of the intermediate frequency semicircle in Fig. 6.

thiazole ring, **Y5**, results in red shift of λ_{max}, albeit with smaller extinction coefficient: **Y2** (λ_{max}=382 nm; ε=2.67×10^{-4} M^{-1} cm^{-1}) versus **Y5** (λ_{max}=413 nm; ε=2.50×10^{-4} M^{-1} cm^{-1}). In comparison, replacement of the pyridine ring in **Y2** with the more electron-rich thiophene ring, **1P-PPS** (Fig. 1),[24] comparable λ_{max} and larger extinction coefficient was observed: **Y2** (λ_{max}=382 nm; ε=2.67×10^{-4} M^{-1} cm^{-1}) versus **1P-PPS** (λ_{max}=380 nm, ε=3.02×10^{-4} M^{-1} cm^{-1}). In contrast, substitution of the pyridine ring in **Y4** (λ_{max}=436 nm, ε=2.51×10^{-4} M^{-1} cm^{-1}) by a thiophene ring, **1P-PSS** (Fig. 1),[24] leads to red shift of absorption as well as larger extinction coefficient (λ_{max}=461 nm, ε=2.71×10^{-4} M^{-1} cm^{-1}). These observations presumably stem from higher resonance energy (32 kcal mol^{-1}) and/or less coplanarity of the pyridine ring with the neighboring aromatic ring in the spacer, which hamper the charge transfer capability.

The absorption spectra of these compounds exhibit a negative solvatochromism, and representative spectra are displayed in Fig. 3 for **Y4**. The λ_{max} values for **Y4** are in the order of dioxane (456 nm)> THF (433 nm)>MeOH (429 nm)>acetone (426 nm)>DMF (418 nm)>MeCN (412 nm). This can be explained by the stronger interaction between the O–H bond of the carboxylic acid with polar solvent molecules, which weakens the O–H bond and decreases the electron-withdrawing nature of the carboxylic group. Similar behavior was reported for metal-free dipolar compounds by us[13b] and others.[25] The compounds emit weakly in the range of 519–553 nm. There is large Stokes shift of the emission ranging from 4829 to 5763 cm^{-1} (Fig. 2b), suggesting that there exists prominent geometrical change between the emission and the ground states in these compounds. Compound **Y2** has the largest Stokes shift (7625 cm^{-1}) among all due to relatively twisted ground-state geometry. The dye **Y1** emits at the shortest wavelength (519 nm) because of its shortest spacer. In comparison, compound **Y4** has longer emission wavelength than **Y1**–**Y3**, in conformity with its longest effective conjugation length.

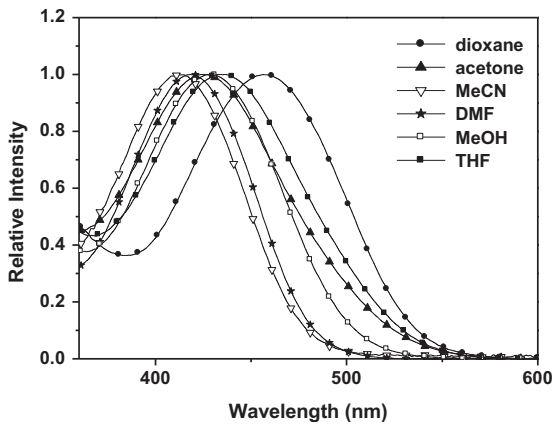

Fig. 3. Absorption spectra of the dye **Y4** recorded in different solvents.

2.3. Electrochemical properties

The electrochemical data of the dyes obtained from cyclic voltammetry (CV) are listed in Table 1 and the differential pulse voltammograms (DPV) are displayed in Fig. 4. All of these dyes exhibit a quasi-reversible one-electron redox process at ca. 500–600 mV, which corresponds to the oxidation of the amino group. The oxidation potentials increase in the order of **Y3** (505 mV)<**Y4** (518 mV)<**Y2**(544 mV)<**Y5** (575 mV)<**Y1** (611 mV). **Y1** has the largest E_{ox} value because its shortest conjugation spacer allows stronger electronic communication between the arylamine and electron-withdrawing 2-cyanoacrylic acid and pyridine. As the spacer becomes longer, there is diminished influence of the acceptor. Consequently, the aromatic segment nearby the arylamine will have more significant influence, and compounds with more electron-donating fluorenyl (**Y3**) or thienyl (**Y4**) groups appear to have smaller E_{ox} than other compounds. As expected, **Y5**, which contains an electron-deficient thiazolyl entity is more difficult to be oxidized than **Y2**.

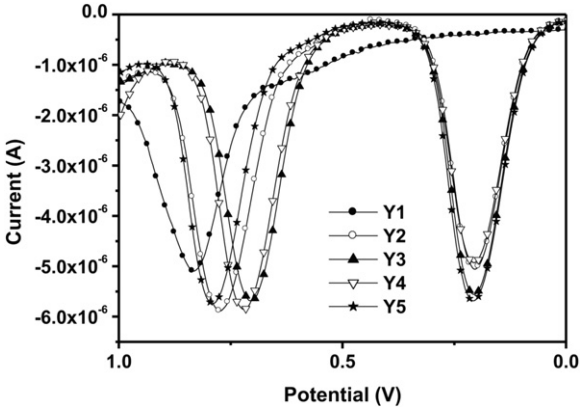

Fig. 4. Differential pulse voltammograms of the compounds recorded in THF.

2.4. Photocurrent–voltage characteristics

The solar cells, with an effective area of 0.25 cm^2, were fabricated with nanocrystalline anatase TiO_2 and sensitized using the organic pyridyl dyes. The electrolyte is composed of 0.05 M I_2/0.5 M LiI/0.5 M

4-*tert*-butylpyridine in acetonitrile solution. The device performance statistics under AM 1.5 illumination are collected in Table 1. Fig. 5 shows both the photocurrent–voltage (J–V) curves and the incident photon-to-current conversion efficiencies (IPCE) of the cells, respectively. All devices fabricated with these dyes exhibited higher quantum efficiencies (65–76%) than N719 in the wavelength range of 400–500 nm. The action spectra (IPCE) of the device based on **Y4** extend even to the near infrared region at 700 nm. As a result, the cell of **Y4** has the highest current density and the overall conversion efficiency (η), reaching 72% of N719-based standard device despite of its somewhat lower V_{OC}. The lower photocurrent of **Y2**- and **Y5**-based device can be rationalized by the significant deviation of the biphenyl spacer from planarity, which decreases the light-harvesting efficiency (shorter absorption wavelength as well as lower absorption intensity) and consequently hampers the cell efficiency. On the other hand, the device **Y3** has current density and cell performance better than the device **Y1**, probably because of better light-harvesting of the fluorene-containing dye.

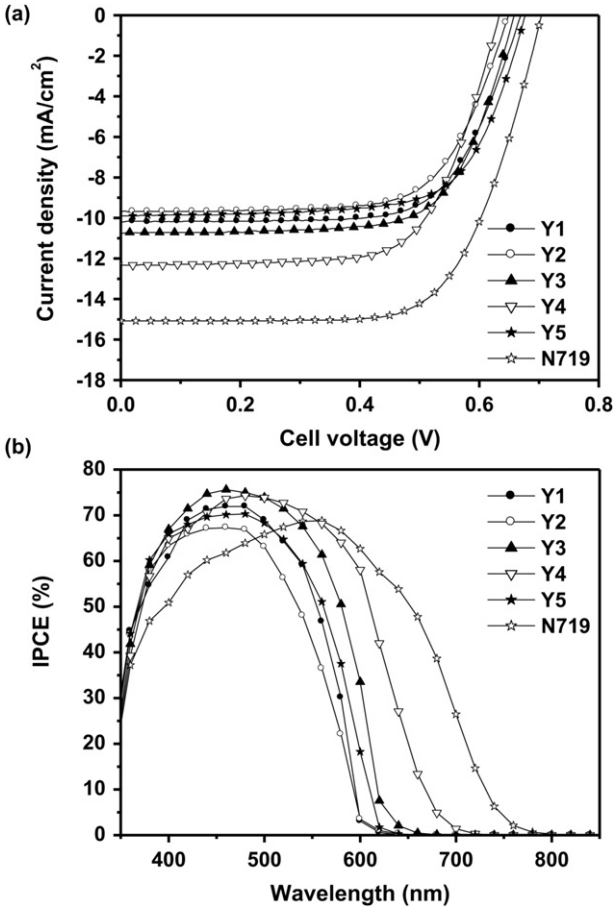

Fig. 5. (a) J–V curves of DSSCs based on the dyes. (b) IPCE plots for the DSSCs.

In order to realize the interfacial charge transfer resistance from the dyes injected into TiO_2, EIS techniques were applied on the DSSCs as shown in Fig. 6 and some of the data are compiled in Table 1. The radius of the intermediate frequency semicircle (1–20 Hz) corresponds to the charge transfer resistance at the TiO_2/dye/electrolyte interface. The lower resistance implies higher electron injection rate from the excited dyes to the TiO_2 and thus resulting in higher photocurrent. The charge transfer resistance decreases in the order of **Y2** (17.3 Ω)>**Y3** (16.5 Ω)>**Y1** (15.9 Ω)>**Y5** (11.6 Ω)>**Y4** (9.8 Ω), which conforms to the order of J_{SC} values except **Y3** and **Y5**. Relatively high photocurrent was observed for the cell of **Y3** in spite of its higher interfacial resistance. In comparison, **Y5** exhibits opposite behavior.

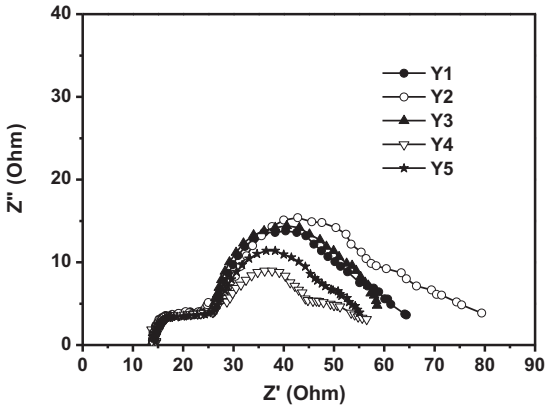

Fig. 6. Electrochemical impedance spectra (Nyquist plots) for the DSSCs measured under illumination (AM 1.5).

These results may be rationalized by different dye densities on TiO_2 surface. The dye loading amount on TiO_2 surface is listed in Table 1. An outstanding dye loading amount was found for **Y3**, and comparatively lower loading was found for **Y5**. Moreover, the high photocurrent performance of **Y4** is resulted from the low charge transfer resistance and high dye loading intensity.

Performance of DSSCs in this study was compared with that based on similar dyes where the pyridyl ring was replaced by a 2,5-thienyl ring in order to evaluate the effect of pyridyl entity. The efficiency of the device from **Y2** is lower than that of **1P**-**PPS** by 7% (comparing to the standard device based on N719). Similarly, the device of **Y4** has an efficiency 9% lower that of **1P**-**PSS**.[24] It is believed that unfavorable twist angle between the pyridyl ring and the neighboring aromatic ring, and a much higher resonance energy of pyridine than thiophene play important roles for deterioration of the cell efficiency. Adopting of 2,5-pyrimidyl ring in the spacer of the sensitizer was reported to have high cell efficiency,[26] indicating that alleviating of the steric congestion in the spacer as well as decreasing the resonance energy of the heteroaromatic ring will be beneficial to the cell performance.

2.5. Theoretical approach

Calculations applying density functional theory at the level of B3LYP/6-31G* were conducted in order to gain further insight into the correlation between the structure and the physical properties as well as the cell performance. Time-dependent DFT results for computation are included in Table S1 (Supplementary data). Fig. 7

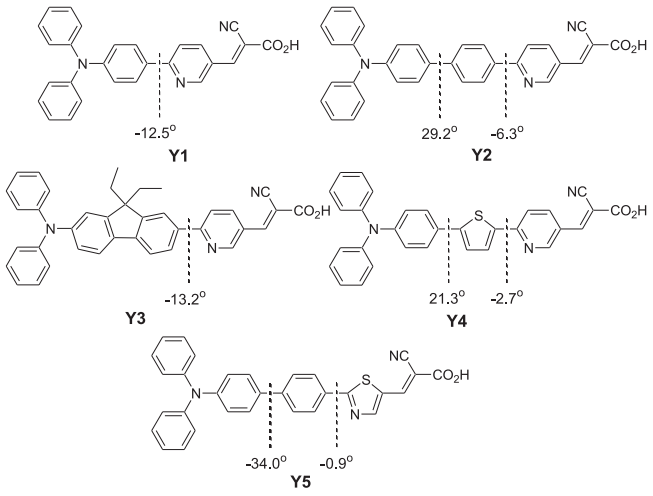

Fig. 7. Dihedral angles between the neighboring units of the dyes.

displays the dihedral angles between neighboring groups in the conjugated spacer. The dihedral angles between the two phenyl rings of the biphenyl spacer appear to be large: 29.2° and 34.0° for **Y2** and **Y4**, respectively. The dihedral angle of the pyridyl ring/phenyl ring is significantly larger than those of the pyridyl ring/thienyl ring and the phenyl ring/thiazolyl ring, and the latter two have negligible values. Fig. 8 displays the HOMO and LUMO orbitals of the compounds with their corresponding energies, and other frontier orbitals are displayed in Fig. S1. $S_0 \rightarrow S_1$ transition mainly comes from HOMO to LUMO and the charge-transfer character of the transition is prominent. The calculated HOMO energies are in the order of **Y3** (−4.99 eV)>**Y2** (−5.07 eV)∼**Y4** (−5.07 eV)>**Y5** (−5.13 eV)>**Y1** (−5.23 eV), which are in the same trend as the results from electrochemical data. For dyes **Y1** and **Y4** the oscillator strength (0.70 and 0.68, respectively) is relatively higher than that in **Y2** and **Y5** (0.44 and 0.39, respectively). This is evidenced in aforementioned calculated coplanarity and perfectly meets the trend found in photophysical data.

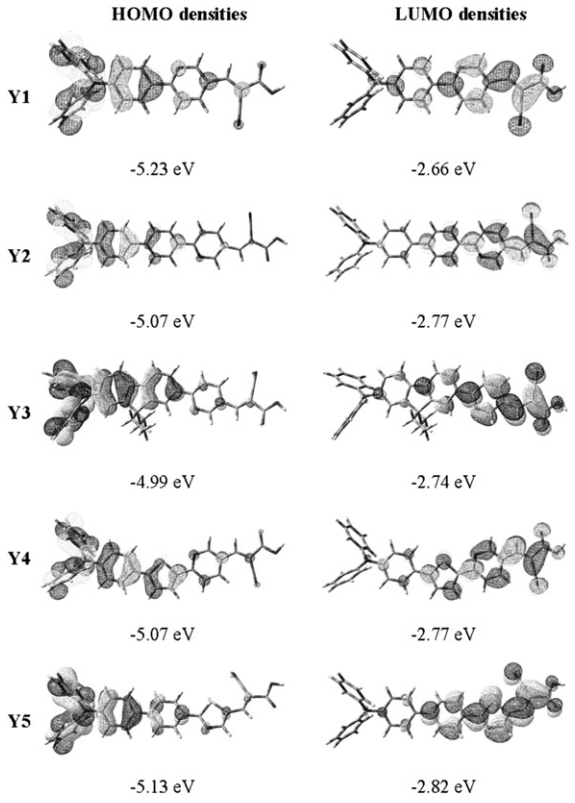

Fig. 8. Selected frontier orbitals and corresponding energy levels of the dyes.

3. Conclusions

In summary, a series of dipolar dyes implanted with pyridine-containing spacer were successfully synthesized and solar cell devices were fabricated and tested. The photo-to-current conversion efficiencies of the cells are in the range of 4.28–5.27%. These values are above 60% of the N719 standard device, with the best efficiency reaching 72% of the standard cell based on N719. The device performance of pyridine dyes falls behind that of thiophene dyes. The somewhat large dihedral angle between the pyridine and the neighboring phenyl group together with the large resonance energy of pyridine hamper effective charge transfer from the donor to the acceptor.

4. Experimental section

4.1. General information

Unless otherwise specified, all the reactions were performed under nitrogen atmosphere using standard Schlenk techniques. All solvents used were purified by standard procedures, or purged with nitrogen before use. ^{1}H NMR and ^{13}C spectra were recorded on a Bruker 400 MHz spectrometer operating at 400.135 MHz and 100.613 MHz, respectively. Absorption spectra were recorded on a Cary 50 probe UV–vis spectrophotometer. All chromatographic separations were carried out on silica gel (60 M, 230–400 mesh). Mass spectra (FAB) were recorded on a VG70–250S mass spectrometer. Elementary analyses were performed on a Perkin–Elmer 2400 CHN analyzer. The TiO_2 nanoparticles and N719 were purchased from Solaronix S. A., Switzerland.

4.2. Synthetic details and characterization

*4.2.1. 6-(4-(Diphenylamino)phenyl)pyridine-3-carbaldehyde (**1a**).* A round-bottom flask weighted with 4-(diphenylamino)phenylboronic acid (1.16 g, 4.01 mmol), 2-bromopyridine-5-carbaldehyde (0.50 g, 2.69 mmol), and tetrakis(triphenylphosphine) palladium (0.38 g, 0.32 mmol) was added 15 mL of toluene, 5 mL of ethanol, and 7 mL of aq Na_2CO_3 (2 M). The resulting solution was heated at 85 °C for 1 day. After the volatiles were removed under vacuum, the resulting residue was dissolved in CH_2Cl_2, washed with brine and dried over $MgSO_4$. The crude product was further purified by column chromatography (silica gel) using CH_2Cl_2 as the eluent to give a yellow powder (0.76 g, Yield 51%). Mass (FAB, *m*/*z*): 350.1 (M^+). ^{1}H NMR (400 MHz, $CDCl_3$): δ 10.07 (s, 1H), 9.04 (d, J_{HH}=1.6 Hz, 1H), 8.16 (dd, J_{HH}=2.0 and 8.4 Hz, 1H), 7.95 (d, J_{HH}=8.8 Hz, 1H), 7.80 (d, J_{HH}=8.4 Hz, 1H), 7.29 (t, 4H), 7.14 (d, J_{HH}=7.6 Hz, 4H), 7.10–7.08 (d, J_{HH}=8.8 Hz, 1H), 7.08 (t, 2H). ^{13}C NMR (100 MHz, $CDCl_3$): δ 190.36, 161.57, 152.60, 150.12, 147.03, 136.28, 130.76, 129.54, 129.21, 128.57, 125.38, 124.0, 122.04, 119.50.

Compounds **2a**–**4a** were synthesized by the same procedures as described above for **1a** using appropriate boronic acids. Compound **2a**: Yield 51%. Mass (FAB, *m*/*z*): 426.2 (M^+). ^{1}H NMR (400 MHz, $CDCl_3$): δ 10.07 (s, 1H), 9.04 (d, J_{HH}=1.6 Hz, 1H), 8.16 (dd, J_{HH}=2.0 and 8.4 Hz, 1H), 7.95 (d, J_{HH}=8.8 Hz, 1H), 7.80 (d, J_{HH}=8.4 Hz, 1H), 7.29 (t, 4H), 7.14 (d, J_{HH}=7.6 Hz, 4H), 7.10–7.08 (d, J_{HH}=8.8 Hz, 1H), 7.08 (t, 2H). ^{13}C NMR (100 MHz, $CDCl_3$): δ 190.61, 162.00, 152.71, 148.05, 147.72, 142.82, 136.67, 136.39, 133.84, 129.96, 129.55, 128.20, 127.96, 127.22, 124.86, 123.75, 123.42, 120.50. Compound **3a**: Yield 58%. Mass (FAB, *m*/*z*): 494.3 (M^+). ^{1}H NMR (400 MHz, $CDCl_3$): δ 10.10 (s, 1H), 9.10 (s, 1H), 8.19 (d, J_{HH}=8.0 Hz, 1H), 8.04 (m, 2H), 7.93 (d, J_{HH}=8.0 Hz, 1H), 7.70 (d, J_{HH}=8.0 Hz, 1H), 7.59 (d, J_{HH}=8.0 Hz, 1H), 7.24 (t, 4H), 7.11 (d, J_{HH}=8.4 Hz, 4H), 7.01 (m, 3H). ^{13}C NMR (100 MHz, $CDCl_3$): δ 190.62, 162.76, 152.73, 152.37, 150.95, 148.26, 148.08, 144.17, 136.50, 136.00, 135.65, 129.72, 129.45, 127.04, 124.32, 123.54, 123.00, 122.00, 121.21, 120.59, 119.62, 119.10, 56.54, 32.83, 8.82. Compound **4a**: Yield 73%. Mass (FAB, *m*/*z*): 432.2 (M^+). ^{1}H NMR (400 MHz, $CDCl_3$): δ 10.01 (s, 1H), 8.93 (s, 1H), 8.10 (dd, J_{HH}=1.6 and 8.0 Hz, 1H), 7.72 (d, J_{HH}=8.4 Hz, 1H), 7.64 (d, J_{HH}=3.6 Hz, 1H), 7.51 (d, J_{HH}=8.4 Hz, 2H), 7.26 (t, 4H), 7.25–7.24 (d, J_{HH}=3.2 Hz, 1H), 7.11 (d, J_{HH}=7.6 Hz, 4H), 7.04 (t, 2H), 7.05 (d, J_{HH}=8.4 Hz, 2H). ^{13}C NMR (100 MHz, $CDCl_3$): δ 190.04, 157.28, 153.06, 149.57, 148.40, 147.44, 141.43, 136.22, 129.61, 129.49, 128.49, 127.53, 126.88, 125.08, 123.70, 123.20, 118.55.

*4.2.2. 2-(4′-(Diphenylamino)biphenyl-4-yl)thiazole-5-carbaldehyde (**5a**).* At nitrogen atmosphere 4′-(diphenylamino)biphenyl-4-ylboronic acid (1.06 g, 2.90 mmol), 2-bromothiazole (0.40 mL, 4.44 mmol), and $Pd(PPh_3)_4$ (0.080 g, 0.070 mmol) were weighted into a round-botton flask. An aqueous solution of Na_2CO_3 (2 M,

7 mL), 15 mL of toluene and 5 mL of ethanol were then added and the resulting solution was heated at 85 °C for 1 day. The solvent was removed under vacuum and the residue was dissolved in CH_2Cl_2, washed with brine and dried over $MgSO_4$. The crude product was purified by column chromatography using CH_2Cl_2 as the eluent to give a yellow intermediate (0.83 g, 71%). ^{1}H NMR (400 MHz, $CDCl_3$): δ 8.00 (d, J_{HH}=8.4 Hz, 2H), 7.86 (d, J_{HH}=3.2 Hz, 1H), 7.63 (dd, J_{HH}=8.4 Hz, 2H), 7.50 (d, J_{HH}=8.4 Hz, 2H), 7.31 (d, J_{HH}=3.6 Hz, 1H), 7.26 (t, 4H), 7.14 (m, 6H), 7.03 (t, 2H). This yellow intermediate (0.70 g, 1.73 mmol) was further dissolved in 20 mL of THF under nitrogen and the solution was cooled using acetone bath to −78 °C, *n*-butyl lithium (1.6 M in hexane, 1.18 mL, 1.90 mmol) was added to the cold solution via syringe in 5 min. After the solution was stirred for 35 min, 0.26 mL of DMF (0.87 mmol) was added all at once. The resulting mixture was stirred for 90 min at −35 °C and was allowed to warm to room temperature and stirred for 30 min. The solution was then quenched by aqueous NH_4Cl, diluted with Et_2O, and washed with brine for several times. The organic extract was dried over $MgSO_4$ and purified by column chromatography using hexanes/ethyl acetate (2:3, v/v) as the eluent. The product was obtained as a yellow powder (0.50 g, 58%). Mass (FAB, *m*/*z*): 432.1 (M^+). ^{1}H NMR (400 MHz, $CDCl_3$): δ 10.02 (s, 1H), 8.41 (s, 1H), 8.05 (d, J_{HH}=8.0 Hz, 2H), 7.67 (d, J_{HH}=8.4 Hz, 2H), 7.50 (d, J_{HH}=8.4 Hz, 2H), 7.27 (t, 4H), 7.12 (d, J_{HH}=8.0 Hz, 6H), 7.05 (t, 2H). ^{13}C NMR (100 MHz, $CDCl_3$): δ 182.20, 175.59, 152.65, 148.38, 147.61, 144.28, 138.86, 133.17, 131.09, 129.59, 127.97, 127.93, 127.28, 125.00, 123.58, 123.49.

*4.2.3. (E)-3-(6-(4-(Diphenylamino)phenyl)pyridin-3-yl)-2-cyanoacrylic acid (**Y1**).* A round-bottom flask equipped with 6-(4-(diphenylamino)phenyl)nicotinaldehyde (0.50 g, 1.43 mmol) and 2-cyanoacetic acid (0.24 g, 2.82 mmol) was charged with 15 mL of MeCN under nitrogen. After adding a few drops of piperidine, the resulting solution was heated at 90 °C for 1 day. Then volatiles of the solution were removed under vacuum. The resulting residue was extracted with dichloromethane and water, dried over $MgSO_4$, followed by column chromatography using in ethylacetate (with 5% of acetic acid) as the eluent. Further recrystallization of the product from acetone gives a red powder (0.22 g, 36%). Anal. Calcd for $C_{27}H_{19}N_3O_2$: C, 77.68; H, 4.59; N, 10.07; Found: C, 77.65; H, 4.67; N, 9.56. HRMS *m*/*z* [M+H$^+$] calcd for $C_{27}H_{20}N_3O_2$: 418.1555; Found: 418.1566. ^{1}H NMR (400 MHz, $CDCl_3$): δ 8.90 (s, 1H), 8.68 (d, JHH=9.2 Hz, 1H), 8.28 (s, 1H), 7.95 (d, J_{HH}=8.4 Hz, 2H), 7.81 (d, J_{HH}=8.4 Hz, 1H), 7.29 (t, 3H), 7.16–7.08 (m, 8H). ^{13}C NMR (75 MHz, THF-d_8): δ 163.681, 160.621, 154.265, 151.482, 151.148, 148.345, 137.479, 132.066, 130.430, 129.277, 126.693, 126.321, 124.841, 122.859, 119.877, 116.480, 105.093.

The syntheses of compounds **Y2**–**Y5** follow the same procedure as that of compound **Y1** using appropriate aldehydes. Compound **Y2**: Yield 46%. Anal. Calcd for $C_{33}H_{23}N_3O_2$: C, 80.31; H, 4.70; N, 8.51; Found: C, 77.98; H, 4.57; N, 7.93. HRMS *m*/*z* [M+H$^+$] calcd for $C_{33}H_{24}N_3O_2$: 494.1868; Found: 494.1878. ^{1}H NMR (400 MHz, $CDCl_3$): δ 8.99 (s, 1H), 8.72 (d, J_{HH}=6.4 Hz, 1H), 8.32 (s, 1H), 8.15 (d, J_{HH}=6.0 Hz, 2H), 7.94 (d, J_{HH}=7.2 Hz, 1H), 7.72 (d, J_{HH}=6.0 Hz, 2H), 7.53 (d, J_{HH}=6.4 Hz, 2H), 7.25 (d, J_{HH}=10.0 Hz, 4H), 7.13 (d, J_{HH}=6.8 Hz, 6H), 7.05 (d, J_{HH}=6.0 Hz, 2H). ^{13}C NMR (100 MHz, DMSO-d_6): δ 172.835, 163.364, 158.497, 154.671, 152.615, 149.326, 147.402, 143.145, 141.611, 137.290, 136.285, 133.252, 130.105, 128.036, 126.958, 124.842, 124.068, 123.912, 123.413, 123.134, 120.510, 117.420. Compound **Y3**: Yield: 33%. Anal. Calcd for $C_{38}H_{31}N_3O_2$: C, 81.26; H, 5.56; N, 7.48; Found: C, 81.36; H, 5.75; N, 7.39. HRMS *m*/*z* [M+H$^+$] calcd for $C_{38}H_{32}N_3O_2$: 562.2494; Found: 562.2508. ^{1}H NMR (400 MHz, acetone-d_6): δ 9.20 (s, 1H), 8.65 (d, J_{HH}=7.6 Hz, 1H), 8.42 (s, 1H), 8.32 (s, 1H), 8.26 (d, J_{HH}=5.6 Hz, 2H), 7.86 (d, J_{HH}=7.6 Hz, 1H), 7.79 (d, J_{HH}=8.0 Hz, 1H), 7.32 (t, 3H), 7.18 (s, 1H), 7.12 (d, J_{HH}=8.0 Hz, 4H), 7.06 (t, 3H), 2.17–1.96 (m, 4H), 0.38 (t, 6H). ^{13}C NMR (100 MHz, THF-d_8): δ 163.820, 161.414, 154.842, 153.055, 151.459, 149.186, 144.937, 138.418, 137.261, 136.792, 130.942, 129.360, 128.462, 126.876, 125.923, 125.245, 124.576, 124.337, 123.618, 123.357, 122.994, 122.846, 121.512, 121.073, 119.885, 116.452, 105.891. Compound **Y4**: Yield 81%. Anal. Calcd for $C_{31}H_{21}N_3O_2S$: C, 74.53; H, 4.24; N, 8.41; Found: C, 74.58; H, 4.18; N, 8.44. HRMS *m*/*z* [M+H$^+$] calcd for $C_{31}H_{22}N_3O_2S$: 500.1432 Found: 500.1444. ^{1}H NMR (400 MHz, acetone-d_6): δ 9.04 (s, 1H), 8.61 (d, J_{HH}=6.8 Hz, 1H), 8.35 (s, 1H), 8.08 (d, J_{HH}=8.8 Hz, 1H), 7.92 (d, J_{HH}=3.6 Hz, 1H), 7.68 (d, J_{HH}=8.4 Hz, 2H), 7.49 (d, J_{HH}=4.0 Hz, 1H), 7.35 (t, 3H), 7.14–7.05 (m, 8H). ^{13}C NMR (75 MHz, DMSO-d_6): δ 163.540, 155.081, 153.405, 151.273, 148.262, 148.022, 147.139, 141.859, 137.079, 130.153, 129.788, 127.356, 127.167, 126.014, 125.066, 124.185, 122.924, 118.910, 116.629, 104.366. Compound **Y5**: Yield 90%. Anal. Calcd for $C_{31}H_{21}N_3O_2S$: C, 74.53; H, 4.24; N, 8.41; Found: C, 74.59; H, 4.15; N, 8.46. HRMS *m*/*z* [M+H$^+$] calcd for $C_{31}H_{22}N_3O_2S$: 500.1432; Found: 500.1441. ^{1}H NMR (400 MHz, acetone-d_6): δ 8.63 (s, 1H), 8.60 (s, 1H), 8.20 (d, J_{HH}=8.4 Hz, 2H), 7.87 (d, J_{HH}=8.4 Hz, 2H), 7.71 (d, J_{HH}=8.4 Hz, 2H), 7.35 (t, 3H), 7.15–7.09 (m, 8H). ^{13}C NMR (75 MHz, DMSO-d_6): δ 173.714, 163.449, 155.898, 148.108, 147.272, 145.131, 143.340, 132.475, 131.533, 130.799, 130.139, 128.229, 128.135, 127.378, 125.022, 124.092, 123.080, 116.531, 102.550.

4.3. Assembly and characterization of DSSCs

The photoanode used was the TiO_2 thin film (12 μm of 20 nm particles as the absorbing layer and 6 μm of 400 nm particles as the scattering layer) coated on FTO glass substrate[27] with a dimension of 0.5×0.5 cm^2, and the film thickness measured by a profilometer (Dektak3, Veeco/Sloan Instruments Inc., USA). A platinized FTO produced by thermopyrolysis of H_2PtCl_6 was used as a counter electrode. The TiO_2 thin film was dipped into the THF or MeCN solution containing 3×10^{-4} M dye sensitizers for at least 12 h. After rinsing with THF or MeCN, the photoanode adhered with a polyester tape of 60 μm in thickness and with a square aperture of 0.36 cm^2 was placed on top of the counter electrode and tightly clipping them together to form a cell. Electrolyte was then injected into the space and then sealing the cell with the Torr Seal® cement (Varian, MA, USA). The electrolyte was composed of 0.5 M lithium iodide (LiI), 0.05 M iodine (I_2), and 0.5 M 4-*tert*-butylpyridine that was dissolved in acetonitrile. The standard cell based on N719 was fabricated and measured under similar conditions. The electrochemical impedance spectra (EIS) of the cells were recorded using a potentiostat/galvanostat (CHI, model 440) under 100 mW cm^{-2} light intensity. The frequency range explored in impedance measurements was 10 mHz–100 kHz with sinusoidal signal (single sine) and an ac amplitude (ΔE_{ac}) of 10 mV. The applied bias voltage was set at the open-circuit voltage of the DSSC, between the Pt counter electrode and the TiO_2-dye working electrode.

4.4. Quantum chemistry computation

The computation was performed with Q-Chem 3.0 software.[28] Geometry optimization of the molecules were performed using hybrid B3LYP functional and 6-31G* basis set. For each molecule, a number of possible conformations were examined and the one with the lowest energy was used. The same functional was also applied for the calculation of excited states using time-dependent density functional theory (TD–DFT). There exist a number of previous works that employed TD–DFT to characterize excited states with charge-transfer character.[29] In some cases underestimation of the excitation energies was seen.[29,30] Therefore, in the present work, we use TD–DFT to visualize the extent of transition moments

as well as their charge-transfer characters, and avoid drawing conclusions from the excitation energy.

Acknowledgements

We thank the Institute of Chemistry, Academia Sinica, and National Science Council, Taiwan, for financial support.

Supplementary data

The details of quantum chemistry computation, cyclic voltammograms and the ^{1}H and ^{13}C NMR spectra are found. Supplementary data associated with this article can be found, in the online version, at doi:10.1016/j.tet.2011.10.038.

References and notes

1. (a) O'Regan, B.; Grätzel, M. *Nature* **1991**, *353*, 737; (b) Hagfeldt, A.; Grätzel, M. *Chem. Rev.* **1995**, *95*, 49; (c) Grätzel, M. *Nature* **2001**, *414*, 338; (d) Grätzel, M. *J. Photochem. Photobiol., A* **2004**, *164*, 3; (e) Grätzel, M. *Chem. Lett.* **2005**, *34*, 8.
2. Robertson, N. *Angew. Chem., Int. Ed.* **2006**, *45*, 2338.
3. (a) Chiba, Y.; Islam, A.; Watanabe, Y.; Komiya, R.; Koide, N.; Han, L. *Jpn. J. Appl. Phys., Part 2* **2006**, *45*, L638; (b) Gao, F.; Wang, Y.; Shi, D.; Zhang, J.; Wang, M.; Jing, X.; Humphry-Baker, R.; Wang, P.; Zakeeruddin, S. M.; Grätzel, M. *J. Am. Chem. Soc.* **2008**, *130*, 10720; (c) Cao, Y.; Bai, Y.; Yu, Q.; Cheng, Y.; Liu, S.; Gao, F.; Wang, P. *J. Phys. Chem. C* **2009**, *113*, 6290; (d) Chen, C.-Y.; Wang, M.; Li, J.-Y.; Pootrakulchote, N.; Alibabaei, L.; Ngoc-le, C.-H.; Decoppet, J.-D.; Tai, J.-H.; Grätzel, C.; Wu, C.-G.; Zakeeruddin, S. M.; Grätzel, M. *ACS Nano* **2009**, *3*, 3103; (e) Yu, Q.; Wang, Y.; Yi, Z.; Zu, N.; Zhang, J.; Zhang, M.; Wang, P. *ACS Nano* **2010**, *4*, 6032.
4. (a) Hara, K.; Sayama, K.; Ohga, Y.; Shinpo, A.; Suga, S.; Arakawa, H. *Chem. Commun.* **2001**, 569; (b) Hara, K.; Kurashige, M.; Dan-oh, Y.; Kasada, C.; Shinpo, A.; Suga, S.; Sayama, K.; Arakawa, H. *New J. Chem.* **2003**, *27*, 783; (c) Hara, K.; Wang, Z.-S.; Sato, T.; Furube, A.; Katoh, R.; Sugihara, H.; Dan-oh, Y.; Kasada, C.; Shinpo, A.; Suga, S. *J. Phys. Chem. B* **2005**, *109*, 15476.
5. (a) Horiuchi, T.; Miura, H.; Uchida, S. *Chem. Commun.* **2003**, 3036; (b) Horiuchi, T.; Miura, H.; Uchida, S. *J. Photochem. Photobiol., A* **2004**, *164*, 29; (c) Ito, S.; Miura, H.; Uchida, S.; Takata, M.; Sumioka, K.; Liska, P.; Comte, P.; Peter Péchy, P.; Grätzel, M. *Chem. Commun.* **2008**, 5194.
6. (a) Ehret, A.; Stuhl, L.; Spitler, M. T. *J. Phys. Chem. B* **2001**, *105*, 9960; (b) Ma, X.; Hua, J.; Wu, W.; Jin, Y.; Meng, F.; Zhan, W.; Tian, H. *Tetrahedron* **2008**, *64*, 345.
7. (a) Wang, Z. A.; Li, F. Y.; Haung, C. H. *Chem. Commun.* **2000**, 2063; (b) Yao, Q. H.; Meng, F. S.; Li, F. Y.; Tian, H.; Huang, C. H. *J. Mater. Chem.* **2003**, *13*, 1048.
8. (a) Velusamy, M.; Justin Thomas, K. R.; Lin, J. T.; Hsu, Y. C.; Ho, K. C. *Org. Lett.* **2005**, *7*, 1899; (b) Kitamura, T.; Ikeda, M.; Shigaki, K.; Inoue, T.; Anderson, N.; Ai, X.; Lian, T.; Yanagida, S. *Chem. Mater.* **2004**, *16*, 1806; (c) Hagberg, D. P.; Edvinssion, T.; Marinado, T.; Boschloo, G.; Hagfeldt, A.; Sun, L. *Chem. Commun.* **2006**, 2245; (d) Xu, W.; Peng, B.; Chen, J.; Liang, M.; Cai, F. *J. Phys. Chem. C* **2008**, *112*, 874.
9. Chen, R.; Yang, X.; Tian, H.; Sun, L. *J. Photochem. Photobiol., A* **2007**, *189*, 295.
10. Ning, Z.; Zhang, Q.; Pei, H.; Luan, J.; Lu, C.; Cui, Y.; Tian, H. *J. Phys. Chem. C* **2009**, *113*, 10307.
11. Hara, K.; Sato, T.; Katoh, R.; Furube, A.; Yoshihara, T.; Murai, M.; Kurashige, M.; Ito, S.; Shinpo, A.; Suga, S.; Sayama, K.; Arakawa, H. *Adv. Funct. Mater.* **2005**, *15*, 246.
12. (a) Li, G.; Jiang, K.-J.; Li, Y.-F.; Li, S.-L.; Yang, L.-M. *J. Phys. Chem. C* **2008**, *112*, 11591; (b) Zhang, G.; Bala, H.; Cheng, Y.; Shi, D.; Lv, X.; Yu, Q.; Wang, P. *Chem. Commun.* **2009**, 2198; (c) Zhang, G.; Bai, Y.; Li, R.; Shi, D.; Wenger, S.; Zakeeruddin, S. M.; Grätzel, M.; Wang, P. *Energy Environ. Sci.* **2009**, *2*, 92; (d) Li, G.; Zhou, Y.-F.; Cao, X. B.; Bao, P.; Jiang, K.-J.; Lin, Y.; Yang, L.-M. *Chem. Commun.* **2009**, 2201.
13. (a) Justin Thomas, K. R.; Lin, J. T.; Hsu, Y. C.; Ho, K. C. *Chem. Commun.* **2005**, 4098; (b) Justin Thomas, K. R.; Hsu, Y.-C.; Lin, J. T.; Lee, K.-M.; Ho, K.-C.; Lai, C.-H.; Cheng, Y.-M.; Chou, P.-T. *Chem. Mater.* **2008**, *20*, 1830; (c) Choi, H.; Baik, C.; Kang, S. O.; Ko, J.; Kang, M.-S.; Nazeeruddin, M. K.; Grätzel, M. *Angew. Chem., Int. Ed.* **2008**, *47*, 327.
14. (a) Lin, J. T.; Chen, P. C.; Yen, Y. S.; Hsu, Y. C.; Chou, H. H.; Yeh, M. C. P. *Org. Lett.* **2009**, *11*, 97; (b) Li, R.; Lv, X.; Shi, D.; Zhou, D.; Cheng, Y.; Zhang, G.; Wang, P. *J. Phys. Chem. C* **2009**, *113*, 7469.
15. (a) Yen, Y. S.; Hsu, Y. C.; Lin, J. T.; Chang, C. W.; Hsu, C. P.; Yin, D. J. *J. Phys. Chem. C* **2008**, *112*, 12557; (b) Li, Q.; Lu, L.; Zhong, C.; Shi, J.; Huang, Q.; Jin, X.; Peng, T.; Qin, J.; Li, Z. *J. Phys. Chem. B* **2009**, *113*, 14588.
16. Zhang, G.; Bala, H.; Cheng, Y.; Shi, D.; Lv, X.; Yu, Q.; Wang, P. *Chem. Commun.* **2009**, 2198.
17. (a) Mishra, A.; Fischer, M. K. R.; Bäuerle, P. *Angew. Chem., Int. Ed.* **2009**, *48*, 2474; (b) Ooyama, Y.; Harima, Y. *Eur. J. Org. Chem.* **2009**, 2903.
18. Ning, Z.; Tian, H. *Chem. Commun.* **2009**, 5483.
19. Chen, C.-H.; Hsu, Y.-C.; Chou, H.-H.; Justin Thomas, K. R.; Lin, J. T.; Hsu, C.-P. *Chem.—Eur. J.* **2010**, *16*, 3184.
20. (a) Zhu, W.; Wu, Y.; Wang, S.; Li, W.; Li, X.; Chen, J.; Wang, Z.-s.; Tian, H. *Adv. Funct. Mater.* **2011**, *21*, 756; (b) Tang, Z.-M.; Lei, T.; Jiang, K.-J.; Song, Y.-L.; Pei, J. *Chem.—Asian J.* **2010**, *5*, 1911; (c) Kim, J.-J.; Choi, H.; Lee, J.-W.; Kang, M.-S.; Song, K.; Kang, S. O.; Ko, J. *J. Mater. Chem.* **2008**, *18*, 5223; (d) Huang, S. T.; Hsu, Y. C.; Yen, Y. S.; Chou, H. H.; Lin, J. T.; Chang, C. W.; Hsu, C. P.; Tsai, C.; Yin, D. J. *J. Phys. Chem. C* **2008**, *112*, 19739.
21. March, J. *Advanced Organic Chemistry*, 4th ed.; Wiley: New York, NY, 1992; p 45.
22. Two papers appeared while this project was ongoing. (a) Lee, M.-W.; Cha, S.-B.; Yang, S.-J.; Park, S. W.; Kim, K.; Park, N.-G.; Lee, D.-H. *Bull. Korean Chem. Soc.* **2009**, *30*, 2269; (b) Nishida, J.-i.; Masuko, T.; Cui, Y.; Hara, K.; Shibuya, H.; Ihara, M.; Hosoyama, T.; Goto, R.; Mori, S.; Yamashita, Y. *J. Phys. Chem. C* **2010**, *114*, 17920.
23. (a) Suzuki, A. *J. Organomet. Chem.* **1999**, *576*, 147; (b) Chinchilla, R.; Najera, C.; Yus, M. *Chem. Rev.* **2004**, *104*, 2667.
24. Chang, Y. J.; Chow, T. J. *Tetrahedron* **2009**, *65*, 4726.
25. Nazeeruddin, M. K.; Péchy, P.; Renouard, T.; Zakeeruddin, S. M.; Humphrey-Baker, R.; Comte, P.; Liska, P.; Cevey, L.; Costa, E.; Shklover, V.; Spiccia, L.; Deacon, G. B.; Bignozzi, C. A.; Grätzel, M. *J. Am. Chem. Soc.* **2001**, *123*, 1613.
26. Lin, L.-Y.; Tsai, C.-H.; Wong, K.-T.; Huang, T.-W.; Wu, C.-C.; Chou, S.-H.; Lin, F.; Chen, S.-H.; Tsai, A.-I. *J. Mater. Chem.* **2011**, *21*, 5950.
27. (a) Huang, C.-Y.; Hsu, Y.-C.; Chen, J.-G.; Suryanarayanan, V.; Lee, K.-M.; Ho, K.-C. *Sol. Energy Mater. Sol. Cells* **2006**, *90*, 2391; (b) Lee, K. M.; Suryanarayanan, V.; Ho, K.-C. *Sol. Energy Mater. Sol. Cells* **2006**, *90*, 2398.
28. (a) Hirata, N.; Lagref, J.-J.; Palomares, E. J.; Durrant, J. R.; Nazeeruddin, M. K.; Grätzel, M.; Di Censo, D. *Chem.—Eur. J.* **2004**, *10*, 595; (b) Durrant, J. R.; Haque, S. A.; Palomares, E. *Chem. Commun.* **2006**, 3279; (c) Shao, Y.; Molnar, L. F.; Jung, Y.; Kussmann, J.; Ochsenfeld, C.; Brown, S. T.; Gilbert, A. T. B.; Slipchenko, L. V.; Levchenko, S. V.; O'Neill, D. P.; DiStasio, R. A., Jr.; Lochan, R. C.; Wang, T.; Beran, G. J. O.; Besley, N. A.; Herbert, J. M.; Lin, C. Y.; Voorhis, T. V.; Chien, S. H.; Sodt, A.; Steele, R. P.; Rassolov, V. A.; Maslen, P. E.; Korambath, P. P.; Adamson, R. D.; Austin, B.; Baker, J.; Byrd, E. F. C.; Dachsel, H.; Doerksen, R. J.; Dreuw, A.; Dunietz, B. D.; Dutoi, A. D.; Furlani, T. R.; Gwaltney, S. R.; Heyden, A.; Hirata, S.; Hsu, C.-P.; Kedziora, G.; Khalliulin, R. Z.; Klunzinger, P.; Lee, A. M.; Lee, M. S.; Liang, W. Z.; Lotan, I.; Nair, N.; Peters, B.; Proynov, E. I.; Pieniazek, P. A.; Rhee, Y. M.; Ritchie, J.; Rosta, E.; Sherrill, C. D.; Simmonett, A. C.; Subotnik, J. E.; Woodcock, H. L., III; Zhang, W.; Bell, A. T.; Chakraborty, A. K. *Phys. Chem. Chem. Phys.* **2006**, *8*, 3172.
29. (a) Vaswani, H. M.; Hsu, C.-P.; Head-Gordon, M.; Fleming, G. R. *J. Phys. Chem. B* **2003**, *107*, 7940; (b) Kurashige, Y.; Nakajima, T.; Kurashige, S.; Hirao, K.; Nishikitani, Y. *J. Phys. Chem. A* **2007**, *111*, 5544.
30. Dreuw, A.; Head-Gordon, M. *J. Am. Chem. Soc.* **2004**, *126*, 4007.